Modelling and data-based identification of heating element in continuous-time domain

Zajic, I. , Iten, M. and Burnham, K.

Modelling and data-based identification of heating element in continuous-time domain

Ivan Zajic[1], Muriel Iten[2] and Keith J Burnham[1]

[1] Control Theory and Applications Centre, Coventry University, Coventry, UK
[2] Civil Engineering, Architecture and Building, Coventry University, Coventry, UK

E-mail: zajici@uni.coventry.ac.uk

Abstract.

A unique data-based and physically meaningful nonlinear continuous-time model of heating element is presented. The model is considered to be of low complexity yet achieving high simulation performance. The physical meaningfulness of the model provides enhanced insight into the performance and functionality of the system. In return, this information can be used during the system simulation and improved model based control designs for tight temperature regulation. The second contribution presented in this work is the parameter estimation of the derived nonlinear model in continuous-time domain itself. For this purpose the application of refined instrumental variable methods has been found to be particularly suitable.

1. Introduction

The paper reports on modelling and data-based identification of a heating element, which preheats the inlet air used by a testbed for testing and modelling of phase change materials (PCM) used in passive air conditioning for sustainable housing applications, for more details see [1]. The main motivation for the work is the actual modelling of the phase change materials itself where a clear parallel between the air being conditioned by a heating element or the PCM based heat exchanger can be found. The later heat exchange process additionally includes nonlinear effects caused by the phase change of the PCM. Therefore the emphasis is given on physical meaningfulness of the derived heating element model with the view of extending this model for later modelling of PCM based heat exchangers.

The presented modelling procedure has been motivated by, but not necessarily strictly follow, the 'data-based mechanistic' approach to identification and modelling of systems [2, 3, 4, 5]. In this approach a parsimonious data-based model is inferred first using statistical system identification tools. Once the model parameters, order and structure are inferred from measured data the obtained data-based model is interpreted in a physical sense. Furthermore, this system identification procedure can be re-iterated such that the physical laws can assist in priming the black-box model structure and *vice versa*. The search for the system model stops when the identified model explains the measured data well and also the model must provide meaningful interpretation of the system in physical terms. In this regard, the final obtained heating element model is unique in its own right, where up to the best knowledge of authors no alike model has been reported in the literature up to date.

The system identification in continuous-time domain is essential so that a direct link between the data-based identified model and physical laws can be established in a straight forward

manner. For this purpose a simplified refined instrumental variable method for linear continuous-time transfer function model identification (SRIVC) has been adopted, see [6, 7] and references therein. The identified heating element model is, however, not linear in structure and resemble a bilinear system models. Therefore, modified SRIVC algorithm capable of parameter estimation of such nonlinear models is used instead [8]. Finally, the nonlinear dynamic behaviour of the identified heating element model throughout the operational envelope is discussed, together with the implications for parameter estimation and simulation of such model, see Sub-section 3.5. Motivated by [9], it will be shown that the dynamic behaviour of the considered nonlinear model at given operating point can be replicated at zero operating point, which has further applications in system identification and simulation of such system models (which are, however, not shown here).

2. Heating element details and system identification set-up

The heating element is part of a larger testbed system for testing and numerical modelling of phase change materials, see [1] for further references. The speed and temperature of air passing around the tested PCM can be freely regulated to meet the demanded test environmental conditions. The air is conditioned by means of the considered heating element which is in a down stream series connection with a cooling unit. Schematic diagram of the heating element installed in the supply duct is provided in Figure 1.

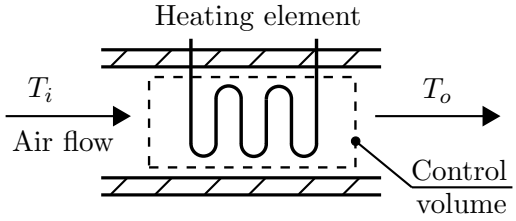

Figure 1. Schematic description of the heating element.

For the system identification purposes the following system inputs are considered: measured inlet air temperature, denoted $T_i(t_k)$ $[K]$, and the air velocity, denoted $v(t_k)$ $[m/s]$. Both system inputs are measured in the centre of the cross sectional area of the supply duct. The outlet air temperature, denoted $T_o(t_k)$ $[K]$, is the assumed system output. The data acquisition experimental set-up has been designed such that the supplied power, denoted $q(t_k)$ $[W]$, to the heating element is constant with the average reading of $q(t_k) = 830$ $[W]$. The inlet air temperate has been altered at random intervals by means of up stream cooling unit; simultaneously the air speed has been stepped up or down by means of altering the supply fan power. The test bed is installed in a large indoor space with approximately constant ambient air temperature, denoted $T_a(t_k)$ $[K]$. The time index (t_k) is chosen to emphasise that the continuous time signals are measured at discrete time index k. The chosen sampling interval is $\tau = 1$ $[s]$, where selection of faster sampling has not been feasible due to the limitations of the data acquisition device.

It is expected to observe that for increasing inlet air temperature the outlet air temperature will also increase and *vice versa*. On the other hand, for increasing air speeds the outlet air temperature should decrease (and the other way around). This can be explained such that for increasing air speeds the air volumetric flow also increases, hence the need for heating, while the heating power is kept constant. For example, the regulation of supply air volume is a common method used in air conditioning of offices and alike spaces [10].

3. Data-based model identification

Having obtained the measured input and output data, being the inlet and outlet air temperatures together with the air velocity, a continuous-time model is identified in a data-based mechanistic manner [3, 4, 5]. The first principles modelling approach, provided in subsequent Section 4, is used to prime the data-based model structure and *vice versa*. The data-based model is used to prime the first principles model, where the suggested model terms are supported by the evidence based on measured data. In overall this iterative procedure confirms the 'appropriateness' of the selected model structure for the data-based identified model and allows a meaningful interpretation in physical terms.

The main outcome of applying the physical laws to prime the data-based model structure has been the selection of two model inputs being the product between the inlet air temperature and air velocity and also the product between the outlet air temperature and air velocity, i.e. $T_i(t_k)v(t_k)$ and $T_o(t_k)v(t_k)$, respectively. This makes the suggested model nonlinear in structure, while still being linear in parameters so that least-squares based model parameter estimation methods can be adopted. However, it should be noted that despite the insight offered by physical laws a purely black-box modelling approach has been also adopted, where various linear and nonlinear regression terms and model orders have been tested with no clear advantage gained in terms of model fit.

3.1. Parameter estimation stage

In order to estimate the model parameters a simplified refined instrumental variable method for linear continuous-time transfer function model identification, SRIVC, has been adopted. The SRIVC algorithm is a direct parameter estimation method, which uses sampled (discrete), noisy, input-output signals and is based on the state variable filter (SVF) approach. The purpose of the optimally selected SVF is twofold, first, to obtain the filtered unknown time derivatives, second, to noise prefilter the measured input-output signals. In the case of white, zero mean, additive measurement noise with Gaussian amplitude distribution the SRIVC algorithm yields asymptotically unbiased statistically efficient (minimum variance) parameter estimates. Another feature of the SRIVC algorithm is the use of instrumental variables (IV), which together with the optimal prefilters form the core of the algorithm. The source of the instrumental variables is the simulated system output. Additionally, the SRIVC algorithm is known for its rapid convergence properties and ease of implementation.

It is important to note that the SRIVC algorithm is designed for linear transfer function model estimation, while the adopted model is nonlinear in structure due to the selection of input signals, cf. (1). Special attention must be paid to the use of instrumental variables, where one of the model inputs contains the measured output. The issue of using SRIVC algorithm in a presence of such a signal product is in detail addressed in [8]. Additionally, the nonlinear model needs to be estimated at its original point of operation, which then implies that a constant offset term must be included in the regression vector of the SRIVC algorithm - this method has been used in this work. Alternatively, in the same manner as in the case of estimation of linear models, it is advantageous to subtract the initial values of measured input-output signal so that the model is estimated at zero operating point. This is not an issue in the case of linear models, however the values of nonlinear model parameters depend on the point of operation. The procedure of tackling this issue is discussed in [8, 9] for the case of identification of bilinear and Hammerstein-bilinear models. Due to the close connection of the considered nonlinear model, cf. (1), with the bilinear model class the same procedure could be adopted.

It should be emphasized, that both system inputs are measurement noise contaminated, i.e. $T_i(t_k)$ and $v(t_k)$. This in effect creates an errors-in-variables identification conceptual scenario, [11], causing a bias in the parameter estimates. However, the SRIVC method uses optimal prefilters which help to attenuate the influence of this input noise on the parameter estimates,

Table 1. Estimated model parameters for model with orders $(n = 2, m = 2)$ are provided on the first two lines, while the parameters for the model $(n = 2, m = 1)$ are provided on the last two lines. The corresponding estimated standard errors are provided in the brackets. The offset terms are $\hat{o} = -279.25$ and $\hat{o} = -122.95$ for models $(n = 2, m = 2)$ and $(n = 2, m = 1)$, respectively.

$\hat{\alpha}_1 \times 10^{-3}$	$\hat{\alpha}_2 \times 10^{-6}$	$\hat{\beta}_0 \times 10^{0}$	$\hat{\beta}_1 \times 10^{-2}$	$\hat{\beta}_2 \times 10^{-4}$	$\hat{\eta}_0 \times 10^{0}$	$\hat{\eta}_1 \times 10^{-2}$	$\hat{\eta}_2 \times 10^{-4}$
8.5257	−9.2335	1.1581	3.8449	1.2031	−0.9620	−3.6187	−1.4548
(0.6627)	(2.3038)	(0.0231)	(0.1194)	(0.1095)	(0.0186)	(0.1004)	(0.1060)
55.026	−92.835	–	9.9837	7.7661	–	−8.5689	−8.3067
(2.0110)	(3.3983)	–	(0.2512)	(0.2835)	–	(0.2070)	(0.2984)

see [7], so that the estimated model may suffice for practical purposes.

The final selected model has two integral terms and a feed-through term, i.e. a second order-like model $n = 2$ with two zeros $m = 2$. The estimated pure time delay is null. It is assumed that any pure time delay has been effectively captured by the dominant dynamics of the model. The final estimated nonlinear model in transfer function-like form is given by

$$T_o(t_k) = \frac{\hat{\beta}_0 s^2 + \hat{\beta}_1 s + \hat{\beta}_2}{s^2 + \hat{\alpha}_1 s + \hat{\alpha}_2}\Big\{T_i(t_k)v(t_k)\Big\} + \frac{\hat{\eta}_0 s^2 + \hat{\eta}_1 s + \hat{\eta}_2}{s^2 + \hat{\alpha}_1 s + \hat{\alpha}_2}\Big\{T_o(t_k)v(t_k)\Big\} + \hat{o} \tag{1}$$

where s denotes a differential operator defined as $s^p x(t) = \frac{\mathrm{d}^p x(t)}{\mathrm{d}t^p}$. The hat symbol over the parameters indicates that these are estimated. The estimated parameters are given in Table 1, where the estimated corresponding standard errors are provided in the parentheses and the estimated offset term is in the table's caption.

3.2. Simulation results and observations

The simulation results are presented in Figure 2. The upper plot shows measured (grey solid line) and simulated (black solid line) outlet air temperature, denoted by $\hat{x}(t_k)$. The middle plot shows the simulation error $e(t_k)$, defined as $e(t_k) = T_o(t_k) - \hat{x}(t_k)$. The lower plot shows inputs $v(t_k)$ (grey solid line) and $T_i(t_k)$ (black solid line). Two model performance criteria are evaluated, namely, the integral of absolute error, denoted IAE [°C], and the coefficient of determination, denoted R_T^2 [%]. The integral of absolute error is defined as

$$IAE = \frac{1}{N}\sum_{k=1}^{N} |e(t_k)| \tag{2}$$

where N is the number of data samples. The IAE criterion then provides an average simulation error in the units of the evaluated output signal (in this case [°C]). The coefficient of determination is defined as

$$R_T^2 = 100\left(1 - \frac{\sigma_e^2}{\sigma_{T_o}^2}\right) \tag{3}$$

where σ_e^2 and $\sigma_{T_o}^2$ are variances of simulation error and outlet temperature, respectively. The R_T^2 criterion then provides a measure of how much of the measured output variance is explained (or captured) by the simulated output variance.

Subsequently, the simulation results with $R_T^2 = 99.68$ [%] and $IAE = 0.1582$ [°C] have been obtained. The evaluated performance criteria indicate an acceptable predictive performance of

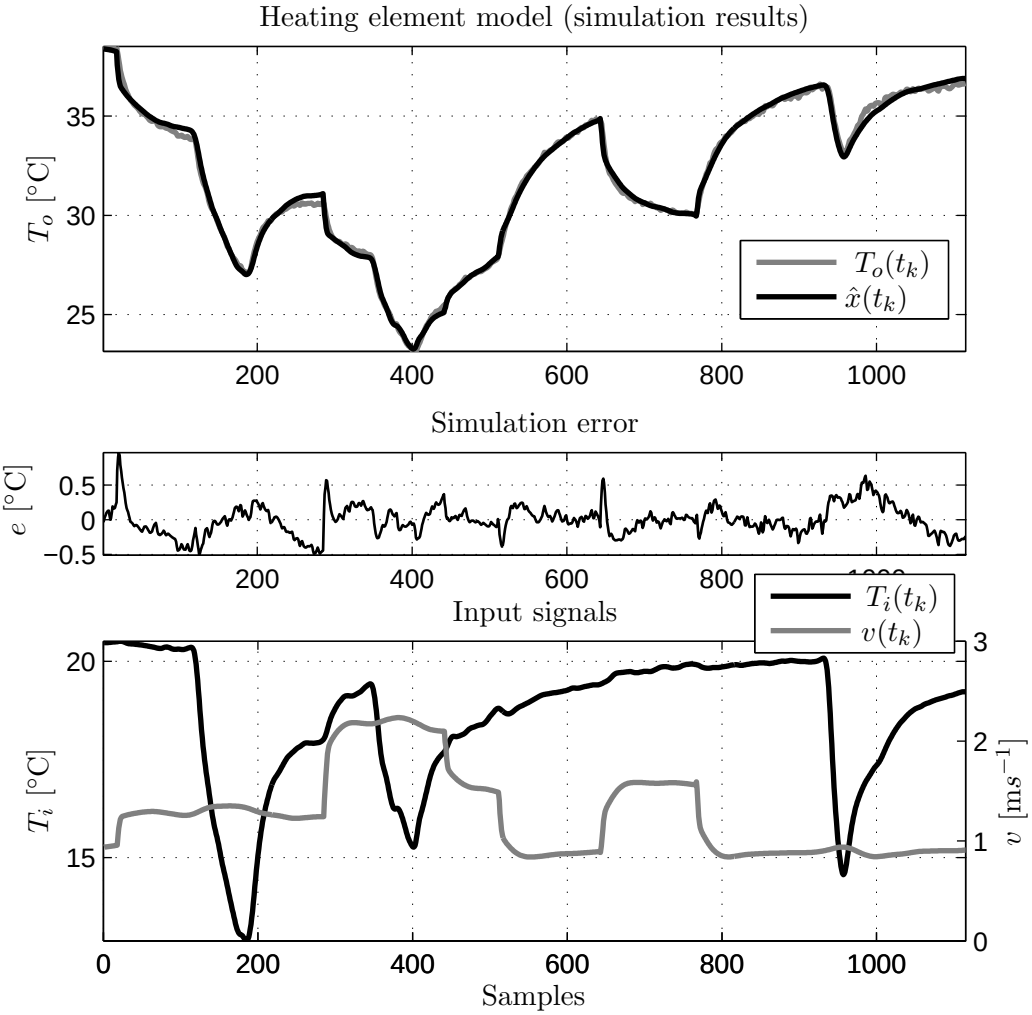

Figure 2. The upper plot shows measured (grey solid line) and simulated (black solid line) outlet air temperatures. The middle plot shows the simulation error defined as the difference between measured and simulated outlet air temperatures. The lower plot shows system inputs, i.e. air velocity (grey solid line) and inlet air temperature (black solid line). Sampling interval is one second.

the estimated heating element model. The simulation error (being also the model residuals), plotted in the middle part of Figure 2, is not a zero mean white noise signal, however that is to be expected in the case of nonlinear model identification. In overall this indicates that the model could not capture all of the deterministic processes caused by the system inputs. It is anticipated that this may have also affected the accuracy of the parameter estimates and that the reported standard errors are probably too optimistic.

Finally, it is instructive to evaluate the nonlinear model (1) dynamics at distinct point of operation. It has been found that the speed of the response depends only on air velocity while the achieved steady-state gain depends on both, the air velocity and the inlet air temperature. Subsequently, linearising the estimated nonlinear model (1) at two stead-state values of air velocity, low and high, respectively, yields two distinct time constants. Considering a low air velocity of $v^* = 0.84$ [ms^{-1}] the two time constants are $T_1 = 55.3$ [s] and $T_2 = 289$ [s]. For

faster air velocity the system response becomes also faster with the two time constants being $T_1 = 41.2$ [s] and $T_2 = 242$ [s].

3.3. Relation to bilinear system models

It is interesting to note that if the inlet air temperature is constant then the identified nonlinear model (1) reduces to a so called bilinear model (a special class of nonlinear models). The characteristic feature of bilinear models is the input dependent dynamic behaviour, see the last paragraph in Sub-section 3.2.

Bilinear models are defined to be *linear* in both state and control when considered independently, with the *bilinearity* (or nonlinearity) arising from coupled terms involving products of the system state and control input. It is this close connection to linear systems, which makes the bilinear models particularly appealing so that many techniques developed for linear systems can be extended and applied to the bilinear case [12]. This has been also one of the reasons why it has been possible to use the SRIVC algorithm which has been originally developed for linear transfer function model estimation, see [8] for more details.

3.4. Reduced order model

The identified second best model in terms of IAE criterion is of the same form as model (1), however without the feed-through terms. The estimated model parameters are provided in Table 1. In order words the two feed-through parameters are $\beta_0 = 0$ and $\eta_0 = 0$ and the model order is $(n = 2, m = 1)$. The obtained performance criteria are $IAE = 0.2269$ [°C] and $RT^2 = 99.47$ [%], which indicates only a slight performance deterioration.

There are two main reasons why the reduced order model might be the preferred option for more practical considerations. The first reason is the reduced computational burden such that the feed-through terms of the original nonlinear model (1) have been inevitably causing an algebraic loop during the model simulation. Secondly, for model based control design purposes it is commonly required that at least one lag (or sample delay) exists between the control input and process output.

Physically meaningful interpretation of the originally estimated nonlinear model (1) is provided in next Section 4. Such interpretation is not provided for the considered reduced order model due to the space limitations. Nevertheless, the first principles model (7), which relates to the originally estimated data-based model (1), can be easily re-arranged to conform to the reduced order model instead. This could be done by combining the energy balance equations (7a) and (7b), hence

$$C\frac{\mathrm{d}T_o(t)}{\mathrm{d}t} = q(t) - v(t)\rho_a A_a c_a \left[T_o(t) - T_i(t)\right] - (UA)_{int}\left[T_o(t) - T_w(t)\right] \tag{4}$$

and leaving (7c) intact. The model parameters in (4) are introduced in the next Section 4 as well as the meaning of (4).

3.5. Non-linear model operation: Simulation at zero operating point

In general, the dynamic and steady-state behaviour of nonlinear models differ throughout the operation envelope. Therefore, if the nonlinear model, such as the identified model (1), is simulated at different operating points a distinct dynamical response will be obtained. This imposes interesting issues in the area of nonlinear system identification. For example, it is not possible to pre-process the measured input-output signals by means of subtracting mean values or initial values prior to parameter estimation and then attempt to estimate the nonlinear model parameters. Of course, this is a common practice when estimating linear transfer function model parameters, however identification of nonlinear models is, in general, not possible in this way (with some exceptions, see [9]).

It is going to be shown, however, that it is possible to simulate the identified nonlinear model (1) at zero operating point while the obtained dynamical response is identical to the one which would be obtained at the original point of operation. This has naturally implications for system identification but also for simulation of nonlinear systems, where the issue of computer simulation initialisation is elevated (initialisitaion of integral terms in particular).

To start with, the input-output signals adopted in the identified model (1) are re-defined or rather substituted with $T_o(t) := T_o(t) + \bar{T}_o$, $T_i(t) := T_i(t) + \bar{T}_i$ and $v(t) := v(t) + \bar{v}$. The input-output signals then comprise the time varying component (deviations) and the steady-state, base-line, component which is denoted by a bar. In the present context the adopted input signals start initially as constant signals and the modelled system is allowed to settle to reach the steady-state. Therefore, the initial values (first sample) of input-output signals are also the base-line components (denoted by the bar). To simplify the following discussion the reduced order model is assumed instead, i.e. $\beta_0 = 0$ and $\eta_0 = 0$ c.f. Section 3.4. Subsequently, if the base-line components are removed (subtracted) from the the input-output signals of model (1) then also the offset term o is effectively removed, see [9], and the following nonlinear, base-line *adjusted*, model can be derived

$$T_o(t) = \frac{B(s)}{A(s|\bar{v})}\Big\{T_i(t)v(t)\Big\} + \frac{E(s)}{A(s|\bar{v})}\Big\{T_o(t)v(t)\Big\} + \frac{B(s|\bar{v})}{A(s|\bar{v})}T_i(t) + \frac{B(s|\bar{T}_i, \bar{T}_o)}{A(s|\bar{v})}v(t) \tag{5}$$

where the constant coefficient polynomials are defined as

$$A(s|\bar{v}) = s^2 + (\alpha_1 - \eta_1\bar{v})\, s + (\alpha_2 - \eta_2\bar{v}) \tag{6a}$$
$$B(s) = \beta_1 s + \beta_2 \tag{6b}$$
$$E(s) = \eta_1 s + \eta_2 \tag{6c}$$
$$B(s|\bar{v}) = (\beta_1\bar{v})\, s + (\beta_2\bar{v}) \tag{6d}$$
$$B(s|\bar{T}_i, \bar{T}_o) = \big(\beta_1\bar{T}_o + \eta_1\bar{T}_i\big)\, s + \big(\beta_2\bar{T}_o + \eta_2\bar{T}_i\big) \tag{6e}$$

The obtained model (5) is then able to replicate the dynamic behavior of the original nonlinear model (1) simulated at the operating point $(\bar{v}, \bar{T}_i, \bar{T}_o)$. Comparing the base-line adjusted model (5) with the original model (1) it is noticed that two new transfer function terms have appeared on the right hand side of (5). These terms compensate for the discrepancy between the response of the original model simulated at operating point $(\bar{v}, \bar{T}_i, \bar{T}_o)$ and the response which would be obtained at zero operating point, i.e. $(\bar{v} = 0, \bar{T}_i = 0, \bar{T}_o = 0)$.

3.5.1. Simulation at zero operating point - An example: The originally identified nonlinear model (1) is simulated using the artificially designed input signals displayed in the lower left plot of Figure 3. The adopted parameters of the reduced order model are given in the lower part of Table 1 with the offset term provided in the caption. The obtained corresponding output is shown in the upper left plot of Figure 3. Consequently, the following base-line values are inferred from the obtained plots, i.e. $(\bar{v} = 1, \bar{T}_i = 20, \bar{T}_o = 36.52)$.

To be able to simulate the nonlinear model at zero operating point the base-line components of input signals are removed; the base-line compensated input signals are provided in the lower right plot of Figure 3. The compensated input signals are then used by the originally identified nonlinear model (1), where the obtained simulated output is shown in the upper right plot of Figure 3 as a grey solid line. The same compensated inputs are also used by the adjusted model (5), where the obtained output is shown as solid black line. The parameters of the adjusted model are calculated using the relations provided in (6) with the previously inferred values of $(\bar{v}, \bar{T}_i, \bar{T}_o)$.

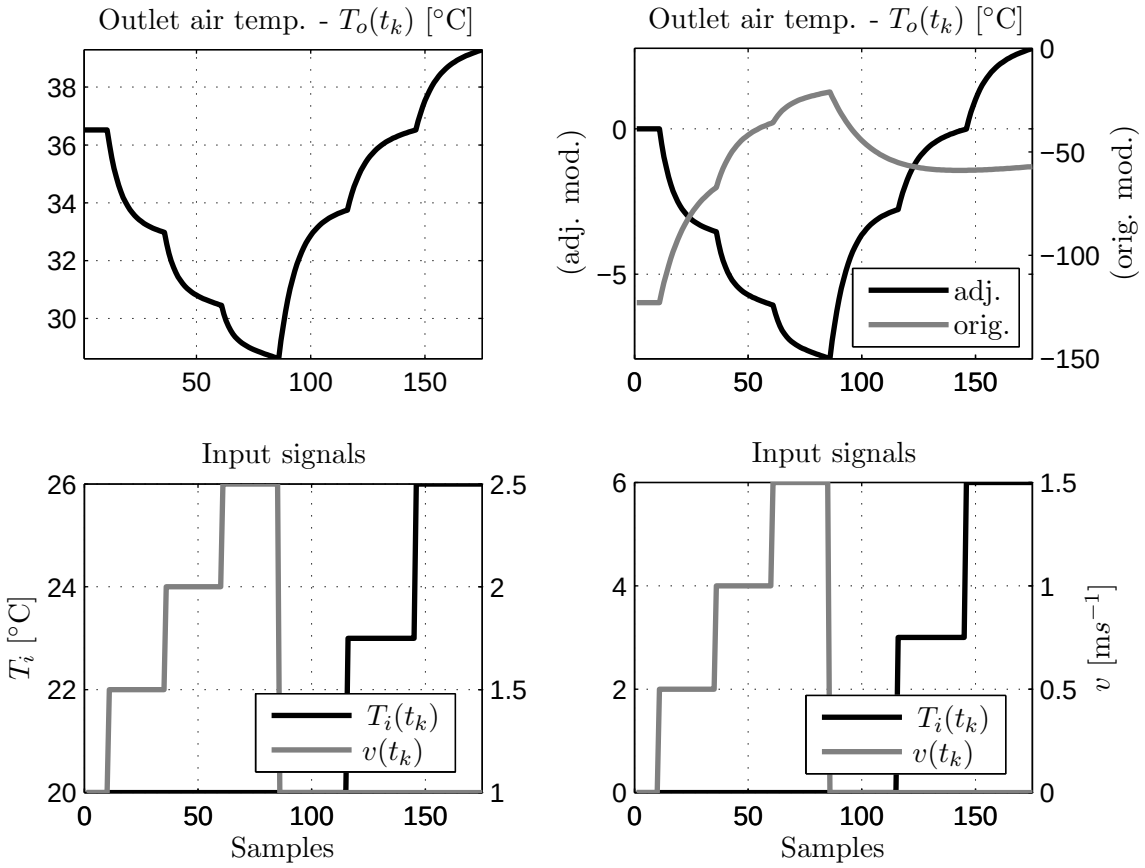

Figure 3. The upper left plot shows simulated outlet air temperature; originally estimated model is used. The lower left plot shows corresponding input signals, i.e. air velocity (grey solid line) and inlet air temperature (black solid line). The upper right plot shows simulated outlet air temperature, where original model (black solid line) and adjusted model (grey solid line) are used. Both simulated outputs are obtained using the base-line compensated input signals shown in the lower right plot, i.e. starting at zero value. The sampling interval is one second.

As expected, it is noticed, that the dynamical response of the original nonlinear model considerably differs at different operating points. It is also observed that the response of the adjusted model (5) is identical to the response of the original nonlinear model obtained at the original point of operation, i.e. $(\bar{v} = 1, \bar{T}_i = 20, \bar{T}_o = 36.52)$, while the adjusted model is simulated at zero operating point, i.e. $(\bar{v} = 0, \bar{T}_i = 0, \bar{T}_o = 0)$. Similarly to [9], it is possible to operate the base-line adjusted model at any operating point (not just zero base-line), while preserving the dynamical response of the nonlinear model from any other point of operation, but this is beyond the scope of the current article.

4. First principles considerations: Mechanistic model interpretation

From the system details provided in Section 2 it is known that the modelled system compose of three main elements, that is the heating element itself, the air control volume and the duct walls. Additionally, the supplied constant heat gain $q(t)$ causes a temperature rise over the heating element. The data-based model (1) indicates, however, that only two dynamical modes

are present (fast and slow mode) and also a feed-through term is clearly present. Therefore, one of the main system components must have negligible thermal capacity.

The air surrounding the heating element is assumed to be perfectly mixed, where the schematic diagram of the system is shown in Figure 1, so that a lumped parameter modelling approach is considered. Under this assumption the outlet air temperature, $T_o(t)$, is assumed to be equal to the mean temperature of the whole control volume. Consequently, the energy balance equations for the heating element, the control volume of air surrounding the heating element and adjacent duct walls, are, respectively, given by

$$C_h \frac{\mathrm{d}T_h(t)}{\mathrm{d}t} = q(t) - (UA)_h \left[T_h(t) - T_o(t)\right] \tag{7a}$$

$$0 = (UA)_h \left[T_h(t) - T_o(t)\right] - v(t)\rho_a A_a c_a \left[T_o(t) - T_i(t)\right] - (UA)_{int} \left[T_o(t) - T_w(t)\right] \tag{7b}$$

$$C_w \frac{\mathrm{d}T_w(t)}{\mathrm{d}t} = (UA)_{int} \left[T_o(t) - T_w(t)\right] - (UA)_{ext} \left[T_w(t) - T_a(t)\right] \tag{7c}$$

where C_h $[J/K]$ is the thermal capacity of the heating element, C_w $[J/K]$ thermal wall capacity (insulated plywood), c_a $[J/kgK]$ is the air specific heat capacity, A_a $[m^2]$ denotes the cross sectional area of the duct, ρ_a $[kg/m^3]$ is the air density. The heat transfer coefficient is denoted by U $[J/m^2K]$ while the product of the heat transfer coefficient and the efficient surface area, A $[m^2]$, through which the heat is transmitted is denoted by $(UA)_h$ $[J/K]$ (heating element), $(UA)_{int}$ $[J/K]$ (inner duct wall) and $(UA)_{ext}$ $[J/K]$ (outer duct wall). The mean temperature of the heating element and wall temperature are denoted, respectively, by $T_h(t)$ $[K]$ and $T_w(t)$ $[K]$. The time index (t) is chosen, emphasising that the signals are not measured but generated by a physical laws based model.

4.1. Remarks on model derivation

The heating element system is represented by three governing nonlinear differential equations (7). The first equation (7a) relates to the energy balance of the heating element itself. It assumed that the inner temperature and the surface temperature of the element are the same and are equal to $T_h(t)$. This is surely simplifying assumption, however considering the small volume of the heating spiral and high temperatures involved, not so unrealistic. It is further assumed that the hating element can be represented as a lumped heat source dissipating all power $q(t)$ into the passing air.

It is assumed that the passing air has negligible thermal capacity so that the heat exchange between the heating element and the air is instantaneous, hence the left hand side of (7b) equals to zero, see e.g. [13]. It is this assumption which supports (implies) the presence of the feed-through terms in data-based model (1). Furthermore, the presence of feed-through terms in (1) can be also interpreted as if not all inlet air is in direct contact with the heating element and that the air just passes around, which surely does occur in practice. Subsequently, the heat transmitted into the passing air must be allowed to dissipate otherwise a first type integrating model would be derived - which is not supported by measured data. It is assumed that the heat loss solely occurs through the walls of the duct, which is expressed by the last energy balance equation (7c).

It should be emphasised that the derived (relatively simple) first principles model (7) is not the only physically feasible interpretation of the data-based model (1), however the model, and the mechanistic interpretation it provides, is considered to be sufficient for the given application. For example, the identified data-based model (1) has two dynamical modes, fast and slow mode, respectively. Based on the first principles model (7) the following mechanistic interpretation can be provided: It can be assumed that the slow mode (time constant is $T \approx 289$ [s]) corresponds to the heat loss through the insulated walls of the duct. Similarly, it can be assumed that the

fast dynamical mode (time constant is $T \approx 55.3$ [s]) relates to the thermal mass of the heating element itself.

4.2. Nonlinear transfer function-like form

For the system identification purposes it is convenient to visualise the set of nonlinear differential equations (7) in a transfer function-like form, from which the interaction between the system inputs and outputs will be clearly visible. In return, this supports the model structure selection of the data-based model.

Using the differential operator s the energy balance equation for the heating element (7a) can be conveniently expressed as follows

$$\left[s + \frac{(UA)_h}{C_h}\right] T_h(t) = q(t) + \frac{(UA)_h}{C_h} T_o(t) \tag{8}$$

Similarly the energy balance equation for the wall (7c) can be arranged as

$$\left[s + \frac{(UA)_{int}}{C_w} + \frac{(UA)_{ext}}{C_w}\right] T_w(t) = \frac{(UA)_{int}}{C_w} T_o(t) + \frac{(UA)_{ext}}{C_w} T_a(t) \tag{9}$$

Subsequently, the set of differential equations (7) is combined by substituting (8) for the unknown heating element temperature $T_h(t)$ in the energy balance equation for air (7b), also the expression (9) is substituted for the unknown wall temperature $T_w(t)$ in (7b). Rewriting and rearranging the resulting expression in a transfer function-like form gives

$$\begin{aligned} T_o(t) = &\frac{\beta_0 s^2 + \beta_1 s + \beta_2}{s^2 + \alpha_1 s + \alpha_2}\Big\{T_i(t)v(t)\Big\} + \frac{\eta_0 s^2 + \eta_1 s + \eta_2}{s^2 + \alpha_1 s + \alpha_2}\Big\{T_o(t)v(t)\Big\} \\ &+ \frac{\gamma_1 s + \gamma_2}{s^2 + \alpha_1 s + \alpha_2} q(t) + \frac{\delta_1 s + \delta_2}{s^2 + \alpha_1 s + \alpha_2} T_a(t) \end{aligned} \tag{10}$$

where the individual model parameters are defined as

$$\begin{aligned} \alpha_1 &= \frac{C_h[(UA)_h(UA)_{int} + (UA)_h(UA)_{ext} + (UA)_{int}(UA)_{ext}] + C_w(UA)_h(UA)_{int}}{[(UA)_h + (UA)_{int}]C_hC_w} \\ \alpha_2 &= \frac{(UA)_h(UA)_{int}(UA)_{ext}}{[(UA)_h + (UA)_{int}]C_hC_w} \\ \beta_0 &= -\eta_0 = \frac{C_hC_w\rho_a A_a c_a}{[(UA)_h + (UA)_{int}]C_hC_w} \\ \beta_1 &= -\eta_1 = \frac{[C_h(UA)_{int} + C_h(UA)_{ext} + C_w(UA)_h]\rho_a A_a c_a}{[(UA)_h + (UA)_{int}]C_hC_w} \\ \beta_2 &= -\eta_2 = \frac{(UA)_h[(UA)_{int} + (UA)_{ext}]\rho_a A_a c_a}{[(UA)_h + (UA)_{int}]C_hC_w} \end{aligned} \tag{11}$$

and

$$\begin{aligned} \delta_1 &= \frac{C_h(UA)_{int}(UA)_{ext}}{[(UA)_h + (UA)_{int}]C_hC_w} \quad \delta_2 = \frac{(UA)_h(UA)_{int}(UA)_{ext}}{[(UA)_h + (UA)_{int}]C_hC_w} \\ \gamma_1 &= \frac{C_w(UA)_h}{[(UA)_h + (UA)_{int}]C_hC_w} \quad \gamma_2 = \frac{(UA)_h[(UA)_{int} + (UA)_{ext}]}{[(UA)_h + (UA)_{int}]C_hC_w} \end{aligned} \tag{12}$$

It is interesting to note that the obtained nonlinear transfer function (10) clearly indicates that the signal products $T_i(t)v(t)$ and $T_o(t)v(t)$ should be considered as system inputs during the

data-based identification stage. Indeed, it has been found in Section 3 that this is the case. The first system input, $T_i(t)v(t)$, directly relates to the amount of heat carried by the inlet air, while the second input, $T_o(t)v(t)$, can be viewed as an internal feedback which assures that as the inlet air speed goes to plus infinity the outlet air temperature converges to the inlet air temperature. Furthermore, considering the model parameters β_i and η_i, $i = 0, 1$ and 2, provided in (11), it can be noticed that assumed physical laws indicate that η_i parameters are equal to β_i parameters however being negative. The estimated $\hat{\beta}_i$ and $\hat{\eta}_i$ parameters provided in Table 1 do clearly confirm this (taking into account the standard error bounds provided by the estimated standard errors).

4.2.1. Mechanistic interpretation of the data-based model - An example: The first principles model (10) does not just provide the information on feasible model structure but also gives us an insight into the estimated data-based model (1). The first principles model suggests that the steady-state gains of the four transfer functions in (10) are related to each other as follows

$$\begin{aligned} \mathrm{SSG}_{vT_i} &= \frac{[(UA)_{int} + (UA)_{ext}]\rho_a A_a c_a}{(UA)_{int}(UA)_{ext}} \\ \mathrm{SSG}_{vT_o} = -\mathrm{SSG}_{vT_i}, \quad \mathrm{SSG}_q &= \frac{\mathrm{SSG}_{vT_i}}{\rho_a A_a c_a}, \quad \mathrm{SSG}_{T_a} = 1 \end{aligned} \tag{13}$$

where SSG denotes the steady-state gain, which has been obtained by setting the differential operator to zero, i.e. $s \to 0$. Considering the identified data-based model (1) it is then possible to infer the value of the steady-state gains (13) as follows

$$\widehat{\mathrm{SSG}}_{vT_i} = \frac{\hat{\beta}_2}{\hat{\alpha}_2}, \quad \widehat{\mathrm{SSG}}_{vT_o} = -\widehat{\mathrm{SSG}}_{vT_i}, \quad \widehat{\mathrm{SSG}}_q = \frac{\widehat{\mathrm{SSG}}_{vT_i}}{\rho_a A_a c_a}, \quad \widehat{\mathrm{SSG}}_{T_a} = 1 \tag{14}$$

Subsequently, recalling that the heating element power has been assumed to be constant as well as the ambient air temperature, i.e. $T_a(t) \approx T_a$ and $q(t) \approx q$, the following must hold

$$\hat{o} = \widehat{\mathrm{SSG}}_q q + \widehat{\mathrm{SSG}}_{T_a} T_a \tag{15}$$

For example, it can be now hypothesised that it is desirable to estimate the heating power q, which is not measured under standard circumstances. Rearranging (15) with respect to 'unknown' q and using the definitions of $\widehat{\mathrm{SSG}}_q$ and $\widehat{\mathrm{SSG}}_{T_a}$ from (14), then

$$\begin{aligned} q &= \frac{\hat{o} - \widehat{\mathrm{SSG}}_{T_a} T_a}{\widehat{\mathrm{SSG}}_q} \\ &= \frac{\hat{\alpha}_2 \left(\hat{o} - T_a\right) \left(\rho_a A_a c_a\right)}{\hat{\beta}_2} \end{aligned} \tag{16}$$

The average measured ambient air temperature was $T_a = 20.48$ [°C]; from the technical sheets the cross section area is $A_a = 0.17$ $[m^2]$, air density $\rho_a = 1.3$ $[kg/m^3]$ and air specific heat capacity $c_a = 1005$ $[J/kgK]$. Subsequently, the estimated heater power is $\hat{q} = 868.5$ $[W]$, which is well in alignment with the measured value of $q = 830$ $[W]$, see system details in Section 2.

5. Conclusions and further work

A unique physically meaningful nonlinear model of heating element has been identified in continuous-time time domain. A relatively high predictive performance of the estimated model has been observed despite its simplicity. Additionally a reduced order model has been introduced

which finds its application in model based control designs. Interestingly, the identified nonlinear model reduces to a so called bilinear model class for constant inlet air temperatures, where such models have been found particularly useful in modelling of heating, ventilation and air conditioning (HVAC) systems by the authors.

The further work will follow two separate but related research streams. Firstly, it is intended to extend the obtained model to include the heating element power as another input. It is then anticipated that such a model will become more universal and will find its application in the area of simulation and control design of HVAC systems. The second work stream will follow modelling and data-based identification of phase change materials (PCM) for air conditioning applications. In these applications the air passes around a heat exchanger filled with PCM. The main difference between such heat exchanger and the considered heating element is that no constant heat power is provided into the heat exchanger. The PCM acts as a heat storage and depending on the air state the heat is either released into the passing air or the air is cooled down. It is assumed that the heat exchange process between the PCM and the passing air can be modeled by the same model as the one obtained in this work, while the inclusion of varying heating power (heat storage) will be required.

References

[1] M. Iten and S. Liu. A work procedure of utilising PCMs as thermal storage systems based on air-TES systems. *Energy conversion and management*, 77:608–627, 2014.

[2] P.C. Young. Data-based mechanistic modelling of environmental, ecological, economic and engineering systems. *Environmental Modelling and Software*, 13:105–122, 1998.

[3] P. C. Young. Data-based mechanistic modelling, generalised sensitivity and dominant mode analysis. *Computer Physics Communications*, 117:113–129, 1999.

[4] L. Price, P. Young, D. Berckmans, K. Janssens, and J. Taylor. Data-based mechanistic modelling (DBM) and control of mass and energy transfer in agricultural buildings. *Annual reviews in Control*, 23:71–82, 1999.

[5] A. Youssef, H. H. Yen, S. E. Özcan, and D. Berckmans. Data-based mechanistic modelling of indoor temperature distributions based on energy input. *Energy and buildings*, 43:2965–2972, 2011.

[6] X. Liu, J. Wang, and W. X. Zheng. Convergence analysis of refined instrumental variable method for continuous-time system identification. *IET Control Theory and Applications*, 5(7):868–877, 2011.

[7] P. C. Young. *Recursive Estimation and Time-Series Analysis: An Introduction for the Student and Practitioner*. Springer-Verlag, 2nd edition, 2011.

[8] I. Zajic. *A Hammerstein-bilinear approach with application to heating ventilation and air conditioning systems*. PhD thesis, Coventry University, UK, 2013.

[9] I. Zajic. and K. J. Burnham. Operating point adjustment procedure for a class of continuous-time bilinear models. In *UKACC Int. Control Conf.*, pages 183–188, Loughborough, UK, 2014.

[10] C. P. Underwood. *HVAC control systems: Modelling, analysis and design*. E.&F.N. Spon, London, 1999.

[11] T. Larkowski. *Extended algorithms for the errors-in-variables identification*. PhD thesis, Coventry University, UK, 2009.

[12] K. J. Burnham, I. Zajic, and T. Larkowski. Review of developments in bilinear systems modelling and control for efficient energy utilization on industrial plant. In *Proc. of 24^{th} Int. Conf. on Efficiency, Cost, Optimization, Simulation and Environmental Impact of Energy Systems*, pages 1856–1870, Novi Sad, Serbia, 2011.

[13] C. P. Underwood. Robust control of HVAC plant I: modelling. *Building services engineering research and technology*, 21:53–61, 2000.